

A Study on the Characteristics of BTA Deep Drilling for Marine Part Carbon and Alloy Steels

Sung-Bo Sim*, Chi-Ok Kim**

* Pukyong National University, ** Pukyong Nat. Univ. Grad. School, Korea

(Received 8 March 2000, accepted 14 April 2000)

ABSTRACT: The term "deep holes" is used to describe the machining of holes with a relatively large length to diameter ratio. The main feature of BTA deep hole drilling is the stabilization of cutting force necessary for the self guidance of the drill head. An additional feature is the cutting tool edges that are unsymmetrically placed on the drill head. There is an increasing necessity to predict the hole geometry and other dynamic stability behavior of deep hole drilling guidance. In this study, the effects of BTA deep hole drilling conditions on the hole profile machined piece are analyzed using domain analysis technique. The profile of deep hole drilled work piece is related to cutting speed, feed rate, chip flow, tool wear, and so on. This study deals with the experimental results obtained during the BTA drilling on SM45C, SM55C carbon steels and SCM440 steels under various cutting conditions, and these results are compared with analytical evaluations.

KEY WORDS: BTA(Boring and Trepanning Association) Drilling, Surface Roughness, Straightness, Roughness, Hole Expansion, Tool Wear

1. Introduction

The deep hole drilling is a process of machining hole that has high length to diameter ratio, typically with hole length ranging from 5 times up to more than 100 times the diameter. It can be classified as BTA(Boring and Trepanning Association) drilling and gun drilling.

BTA drilling differs from the conventional gun drilling in tip configuration, fluid induction and chip removal. However, they have similar guiding and supporting bearings. The tool for deep hole drilling is mounted in the tubular shank. The cutting tip cuts the workpiece in the circular direction and moves in the direction of tool axis.

The tools used for deep hole drilling is a specially manufactured horizontal lathe that has a large flux and high pressure fluid system. It can produce accurate deep as well as shallow holes with good surface finish at high production rates. The BTA drilling has been studied by Beisner, Pearson, et al.¹⁻³⁾

This study investigates the surface roughness, straightness, roundness and hole expansion of the hole and tool wear etc. in single tube system BTA drilling for SM45C, SM55C carbon steels and SCM440 alloy steel.

2. Experimental Method

2-1. Experimental Apparatus

Table 1 is the list of apparatus that were used including the deep hole drilling machine. The workpiece was fixed on the table with angle type device, and the tool is installed in the rotating

type CNC deep hole drilling machine, and the coolant used was machining oil under 2.5MPa fluid pressure.

2-2. Workpiece and Tool

The workpiece and tool in this experiment used are shown in Table. 2 The chemical compositions, mechanical properties are shown in Table 3 and Table 4 respectively. Heat treatment and lathe working performed for the purpose of removing internal stress were adequate for the experiments. Fig. 1 shows the BTA drilling machine. Fig. 2 shows the BTA drilled workpieces.

Fig. 3 shows a schematic diagram of the experimental apparatus with BTA machine tool and alloy measuring instruments.

Fig. 4 shows the BTA deep hole drilling process controlled by CNC macro program. Some workpieces were drilled according to I, II, III and IV tooling routes, and others I, II, and V tooling routes. (For further details on the experimental apparatus, see proceedings of '97, '98, '99 ISOPE conferences)

3. Experimental Result and Consideration

3-1. Surface Roughness

The surface roughness R_{max} of SM55C carbon steel with BTA drilled deep hole is shown in Fig. 5, which shows the plot of R_{max} below $15\mu\text{m}$ value. This result is appropriate for the desired machining efficiency. It is considered that the result indicates efficient burnishing by the guide pad, and that the reaming or post machining is unnecessary. Also the lowest observed surface roughness of $5\mu\text{m}$ can be considered for application in micro-

Table 1 List of experimental apparatus

No	Name	Model	Maker
1	Deephole drilling machine	BTA 1500 CNC	Shin Il M/C co
2	Surface roughness tester	ISO/6	Taylor Hobson
3	Roundness tester	RTH TR 150	Taylor Hobson
4	SEM	S-2700	Hitachi
5	Optical microscope	RM-TH-10	Meiji techo
6	BTA deep hole drill	Ø19.25mm	Korea Tungsten
7	Inside micrometer	5~25mm	Mitutoyo
8	Surface roughness tester	M10-0003	Taylor Hobson
9	3D measuring machine	EC-3200 PA 600A	Kosak Seimitsu
10	Tool dynamometer	9271A	Kistler
11	Charge amp.	5007	Kistler
12	Recorder	MR-30	TEAC
13	PC	IBM-AT 586	Sam Bo
14	Labcard	PCL-818	Advantech Co.
15	Oscilloscope	5504	Hung Chang

Table 2 List of tool and workpiece

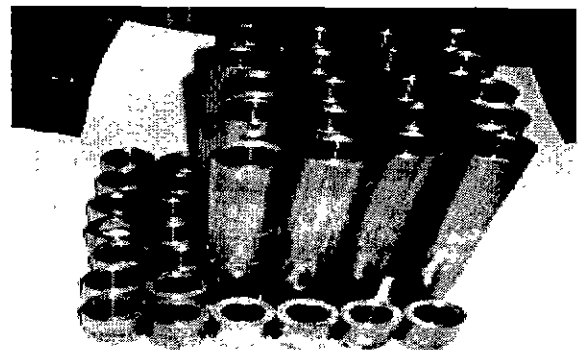
Tool diameter	Tool material	Work piece size	Work piece material
Ø19.25	P30	Ø40×200	SCM440
Ø19.25	P70	Ø40×200 Ø50×60	SM45C
Ø17.1 Ø18.1	P20	Ø40×L	SM55C

Table 3 Chemical composition of workpiece(Wt.%)

Material	C	Mn	Si	P	S	Cr	Ni	Mo	Co
SCM440	0.38	0.73	0.25	0.028	0.17	1.14	0.09	0.17	0.14
SM45C	0.47	0.65	0.31	0.013	0.028				
SM55C	0.55	0.75	0.25	0.025	0.030				

Table 4 Mechanical properties of workpiece

Material	Yielding strength	Tensile strength	Hardness	Elongation
	MPa	MPa	BHN	%
SCM440	86	105	310	15
SM45C	365	596	200	19.8
SM55C	539	735	232	10.0

**Fig. 1** BTA deephole drilling machine with experimental device**Fig. 2** Experimental BTA deep hole drilled workpiece

machining components in industry. In other words the initial cutting region of new BTA drill is suitable for high quality components. But the region having greater than 1000 mm BTA drilling depth is also suitable for application in coolant hole in injection moulding tool, because the hole of injection moulding tool is longer than 1000mm usually and rough inside wall surface and the heat exchange tube seat needs also this drilling method so on.

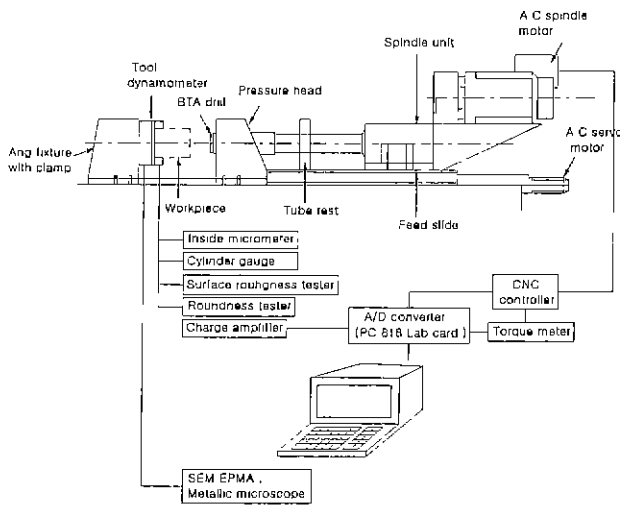
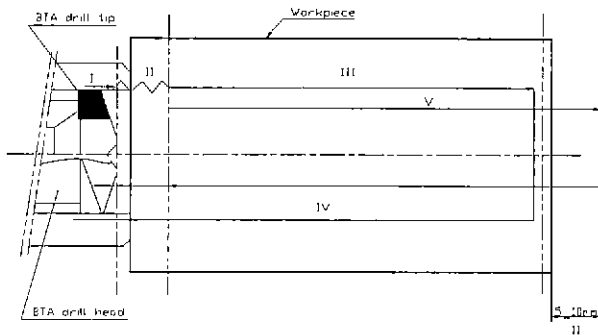


Fig. 3 Schematic diagram of the experimental apparatus



- I : Initial tool location (-1 mm)
- II : Decelerating location
- III : Normal cutting location
- IV : Returning route often drilling in workpiece lead end
- V : Penetrating the hole and returning route

Fig. 4 Configuration of BTA drilling process and route

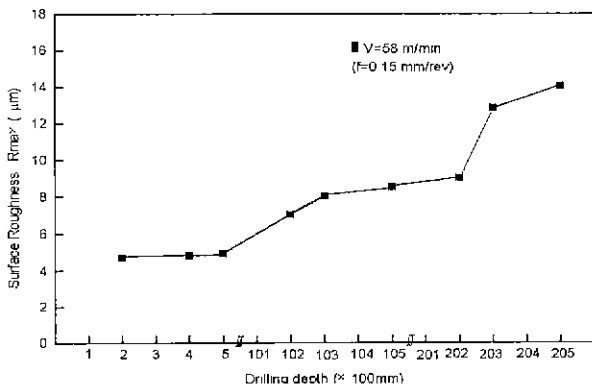


Fig. 5 Relation between surface roughness and drilling depth with BTA drill (SM55C, $\text{Ø}18.1$)

Fig. 6 shows the background point of the above described phenomena. In this figure, "before burnishing" means nonguide pad action which is the region that is acted by only the BTA drill tip edge, and "after burnishing" means the guide pad acted zone, assuming the guide pad performs perfectly.^{4,5)}

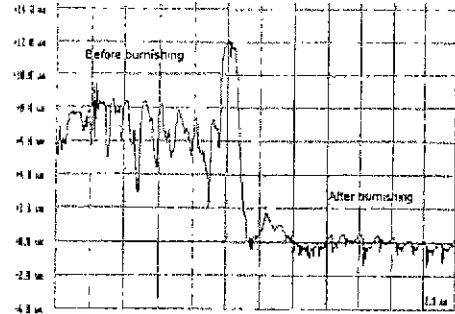


Fig. 6 Surface profile of multi-edge BTA drilled hole ($\text{Ø}18.1$, $V=70$ m/min, $f=0.15$ mm/rev)

Fig. 7 shows one of the SCM440 alloy steel's surface roughness measured by surface roughness instrument (Taylor-Hobson model). In this figure, we see that the surface is very smooth along the pin point moving trace.

As a result, R_a for at this cutting speed and feed rate, the hole surface roughness is below $0.65\mu\text{m}$ except for one work piece. This result is adequate for machining efficiency purpose.

We can consider that this the result indicates that the burnishing is done efficiently by the guide pad activities, and that reaming or post machining is unnecessary. At cutting speeds of 75, 80, 85, 95, 100 m/min, the surface roughness was found to be below $R_a=0.40\mu\text{m}$. value except for one workpiece.

Also, using the same feed rate under the cutting condition 0.14 mm/rev, the finest surface roughness value was found to be below $0.60\mu\text{m}$ R_a value.

Consequently, this is considered to be suitable for the field. This result comes from plastic deformation of BTA drill's guide pad.

We presume that the plastic deformation energy is minimized. Therefore, we can recommend that the feed rate 0.10, 0.14, 0.18 mm/rev, cutting speed 75, 80, 90 m/min are suitable cutting conditions for the industrial.⁶⁾

In Fig. 8 the drill has moved forward by one unit time at given feed rate, and the pads have displaced area DEFG. Plastic flow occurs both before and after the area EHII, and rises above the cut surface to form recreate the ridge, and in the after direction the plastic flow tends to fill in the previous indentation area KLGM as indicated by the traces. Thus:

$$\text{Area}(DEFG) = \text{Area}(EHII) + \text{Area}(KLGM)$$

$$= A_B \approx f\delta \tag{1}$$

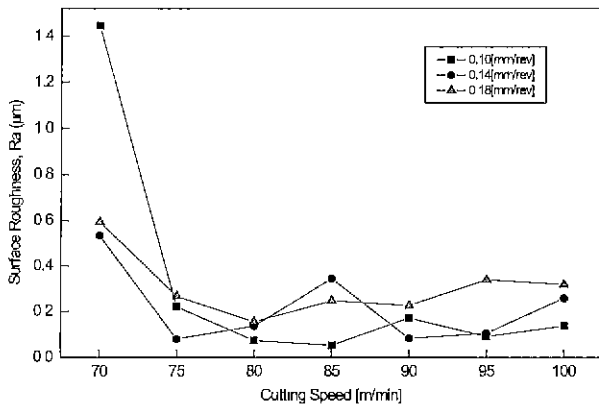


Fig. 7 Relation between Surface Roughness and Cutting Speed for BTA drilled workpiece(SCM440, Ø19.25.)

Studies using scanning electron micro scope show that plastic flow occurs in the material because the same surfaces prior to the deformation, remain as the surface after deformation, i.e. surface GDE is transposed to GFE. This plastic flow causes high pressures at the pads. Previous work(Weber 1978) has shown that approximately 35% of the drilling torque(T_D), hence the power, is expended at the pads, and the remaining 65% at the cutting edge. However, not all the pad torque is expended in burnishing because friction forces are also present along the remainder pad surface.^{6,7)}

Weber found the burnishing torque to be 15% of the drilling torque whereas Griffiths^{2,9)} found it was 24%. It is noted that the methodologies they used in measuring these values as well as their drilling conditions were very different.

For convenience a value of 20% is used and thus the specific burnishing pressure (K_B) acting on the pads can be calculated from next formula.

$$K_B = \frac{2 T_B}{D f \delta} \quad (2)$$

where, f : feed rate, δ : Hole magnification amount

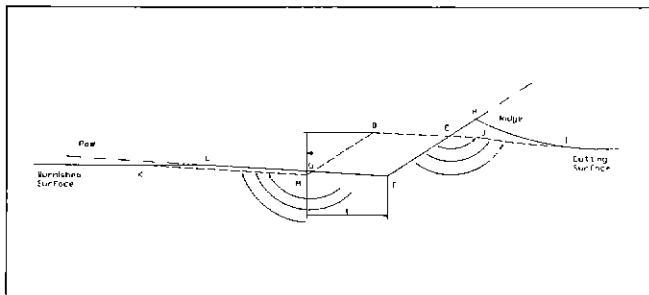


Fig. 8 Schematic representation of deformation cycle by guide pad

3-2. Straightness

The straightness on the BTA deep drilling is related to the alignment and drill tube bending during drilling.

Fig. 9 shows the geometric accuracy measured from BTA drilled hole sample.

In this sample the straightness is found to be 337 in 117 region of the BTA drilled workpiece. The other workpieces were found to field similar results as this sample.

This satisfactory result is obtained because of the fine installation at tool alignment of our BTA drilling machine.

Fig. 10 shows the effect of deep hole drilling condition's on the straightness.

In this figure, we can see that at cutting speed of 85~90m/min, feed rate 0.18mm/rev, the straightness is less than 10μm. Also, it is noted that the deep hole drilling data is kept confidential in field. Therefore its drilling condition is appropriate to select that fine straightness only needs to the machinery components. The tool alignment is maintained to its best possible based on the operator's experience and the available technology.

Fig. 11 shows the straightness sampling measured by Taylor Hobson instrument. In this figure, We can evaluate the trend of straightness value and its relationship to the tool penetrating in deep hole that is consistent with BTA drill head behaviors.

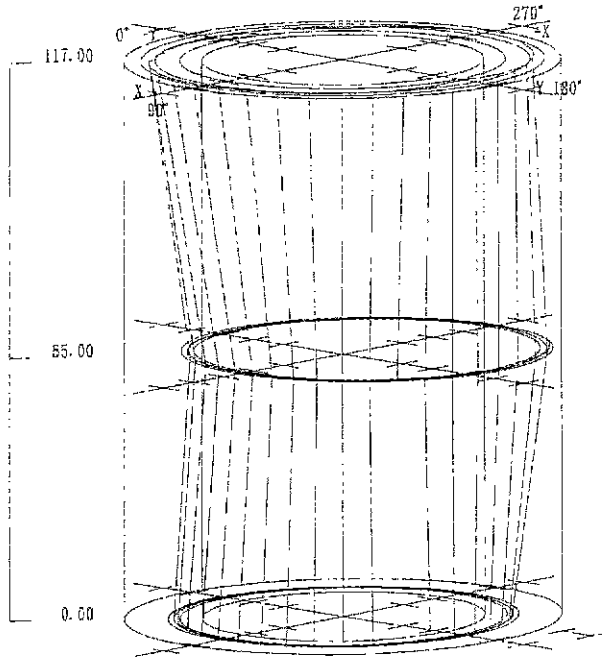
3-3. Roundness

Fig. 12 shows roundness data obtained under fixed cutting conditions (workpiece material SM45C) such as tool diameter ϕ 19.25, feed $f=0.02$ mm/rev, cutting speed $V=60$ m/min to 120m/min, axial depth of deep hole 200mm, The average roundness was shown. In this figure, most of the data are lower than 9μm. With higher cutting speed $V=110$ m/min, the roundness value decreases to less than 4μm. These results indicate that increasing BTA drill's RPM will improve the roundness property.

Fig. 13 shows the experimental results of roundness obtained from BTA deep hole drilling of SM55C. In this figure, the best condition is a cutting speed of 60m/min and a feed rate of 0.2mm/rev. The roundness in both case was below 13μm. There was no problem with the accuracy of the round hole profile. Comparing these two drilling conditions, drilling speed $V=70$ m/min yields slightly better hole profile in term of roundness than that at $V=58$ m/min at the same feed rate of $f=0.15$ mm/rev. Therefore, to improve roundness we can consider the utility of higher cutting speed and lower feed rate.

Fig. 14 shows the experimental results on roundness obtained from BTA deep hole drilled workpiece of SCM440. In this figure, the best results are obtained with the condition of cutting speed $V=90$ m/min and feed rate $f=0.18$ mm/rev.

The roundness of all these experiments appeared to be below 45μm.



Cylindricity : 36.3 μm
 * Straightness : 33.7 μm
 Roundness : 9.9 μm
 Deviation : 8.4 μm

Fig. 9 Geometric accuracy of BTA drilled hole (SM45C, ϕ 19.25, $V=65\text{m/min}$, $f=0.15\text{mm/rev}$)

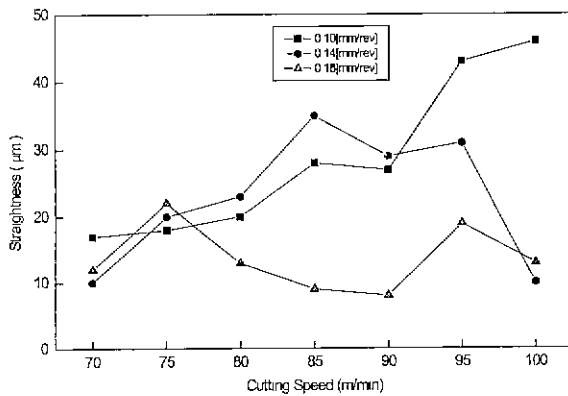


Fig. 10 Relation between straightness and Cutting Speed for BTA drilled workpiece

The experiment was performed without any problem in hole profile accuracy⁴⁻⁸⁾. The roundness data will be further discussed in the context of lobe profile below.

3-4. Profile and Creation of Lobe

Fig. 15(a), (b), (c) and (d) shows the experimental lobe profile

measured from BTA drilled holes. Fig. 15 (a), (b) were obtained at cutting speed 71m/min, feed rate 0.165m/rev of SM45C carbon steel.

Fig. 15 (c) was the result at cutting speed $V=70\text{m/min}$, feed rate $f=0.18\text{mm/rev}$ on SCM440 alloy steel workpiece deep drilled hole.

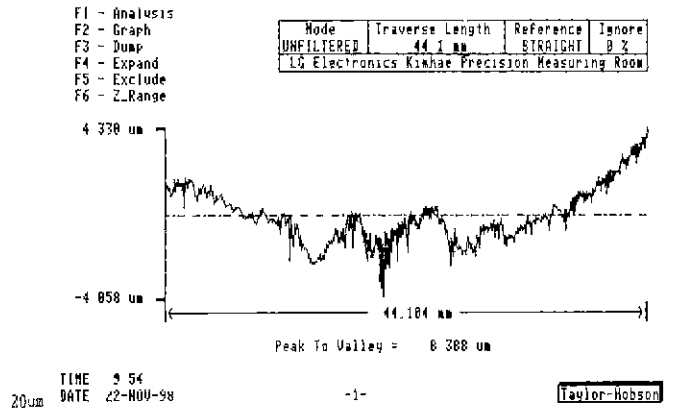


Fig. 11 Sample of straightness measurement (SCM440, ϕ 19.25, $V=90\text{ m/min}$, $f=0.18\text{ mm/rev}$)

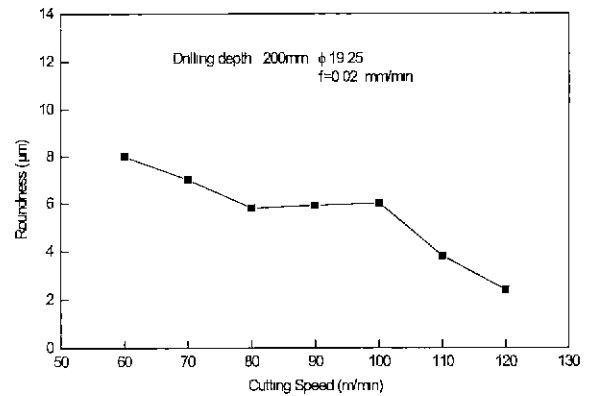


Fig. 12 Relation between roundness and cutting speed with BTA drill(SM45C)

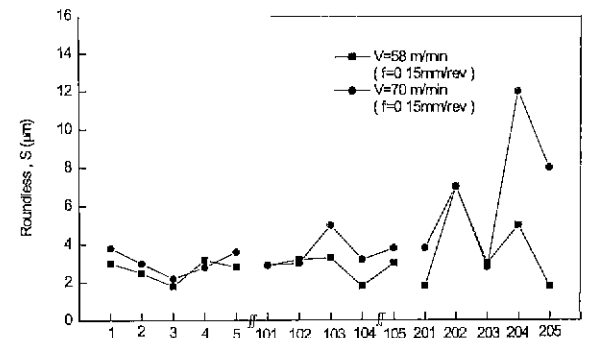


Fig. 13 Relation between roundness and drilling depth with BTA drill (SM55C, ϕ 17.1)

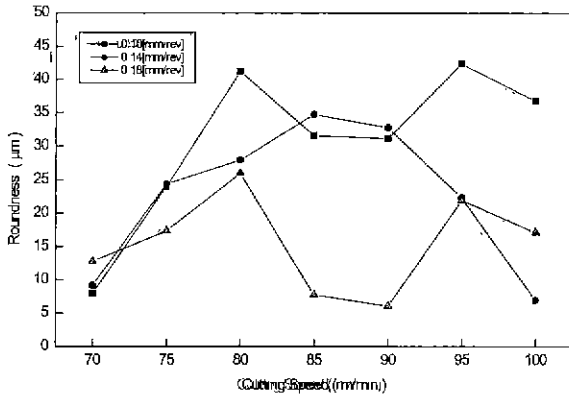


Fig. 14 Relation between Roundness and Cutting Speed for BTA drilled workpiece(SCM440, φ 19.25)

Fig. 15 (d) was the result at cutting speed V=75m/min, feed rate f=0.14mm/rev on SCM440 alloy steel workpiece deep drilled hole.

The majority of the tested BTA drilling conditions results in 2~8 lobes in the deep hole profile. These results indicate the occurrence of variant tool vibration. The drilling operation was performed with high accuracy utilizing the long experience of skilled operators and the maintenance of excellent machining conditions. The lobe profile formed can be described using the following formula.

$$|R| = \sqrt{X^2 + Y^2}$$

$$= \frac{1}{2} \sqrt{[D_a^2 + D_t^2 + 2 D_a D_t \cos((nz-1) \omega_t t + (\psi_a - \theta_a))]} \quad (3)$$

The above formula is for the ease that |nz-1| lobes are formed. In this case,

- ψ_a, θ_a : initial phase
- n : integer
- D_t : tool diameter
- D_a : revolution diameter
- ω_t : tool angular velocity
- ω_a : tool axis angular velocity
- Z : number of cutting edges

\vec{R} : vector locus by work piece lobe radius.

From the above formula, we can calculate the theoretical results as described in proceedings of ISOPE conference '97 '98 '99 by S. B, Sim.^{4,7,8,9,10)}

3-5. Hole Magnification

Fig. 16 shows the amount of hole magnification on BTA drilled hole. In this figure, the highest magnification obtained is about 60µm and the lowest amount is 20µm. These results are

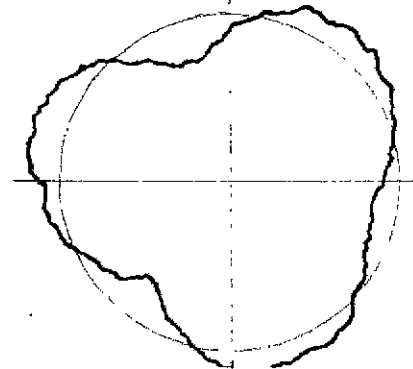
similar to the theoretically calculated hole expansion shown in Fig. 17, 18. The theoretical equation used in these calculation is as follows.²⁻¹⁰⁾

$$\Delta D = \left(\frac{K_s D}{2 H_B W} - C + \frac{1}{4} \right) f \tan \lambda \quad (4)$$

Where,

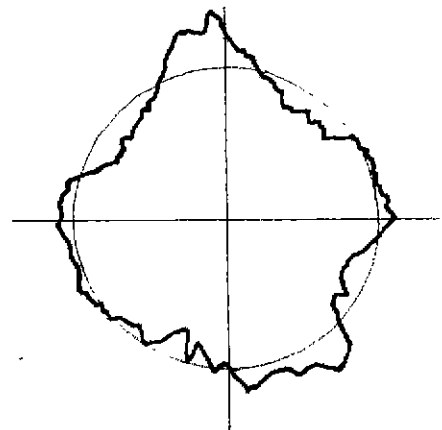
- f : feed rate
- ΔD : amount of hole
- H_B : hardness of workpiece
- λ : contact angle of guide pad on the workpiece
- D : BTA drill diameter
- K_s : specific cutting force
- W : Width of guide pad

C = $\frac{l_2}{f}$: contact length of guide pad on drilling hole surface



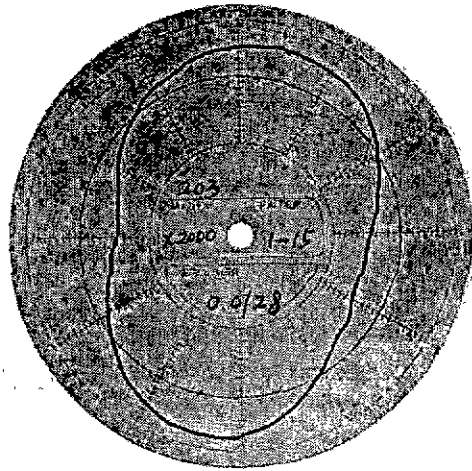
3 lobes

Fig. 15(a) Experimental locus of lobe profile of BTA drilled hole(SM45C φ 19.25 V=71m/min, f =0.165mm/rev)



4 lobes

Fig. 15(b) Experimental locus of lobe profile of BTA drilled hole(SM45C φ 19.25 V=71m/min, f =0.165mm/rev)



2 lobes

Fig. 15(c) Experimental locus of lobe profile of BTA drilled hole(SCM440, ϕ 19.25 V=70m/min, f =0.18mm/rev)

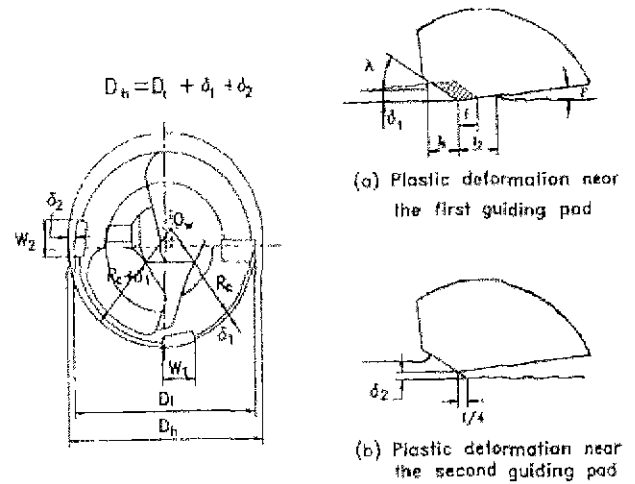
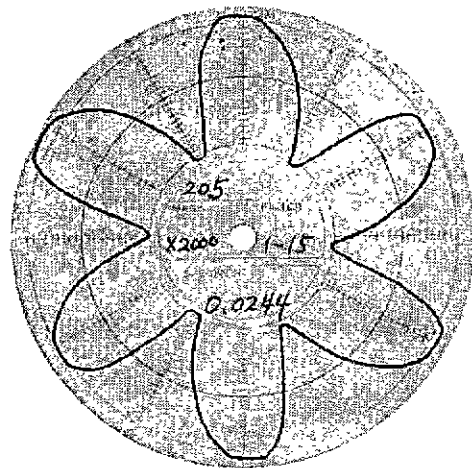


Fig. 17 Hole magnifying mechanism with burnishing guide pad



6 lobes

Fig. 15(d) Experimental locus of lobe profile of BTA drilled hole(SCM440, ϕ 19.25 V=75m/min, f =0.14mm/rev)

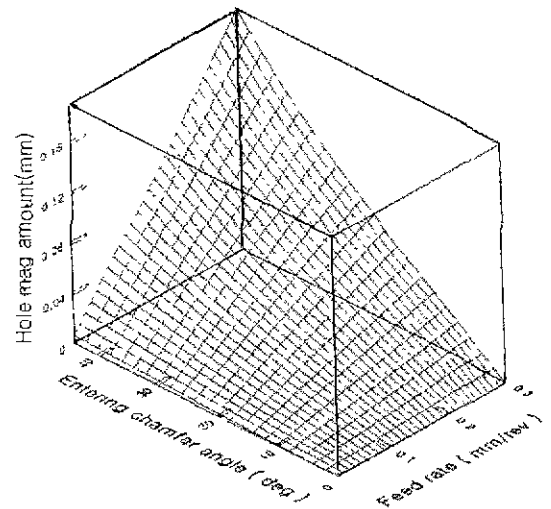


Fig. 18 Calculated result of magnified hole size plotted against entering chamfering angle and feed rate (SM55C)2,5)

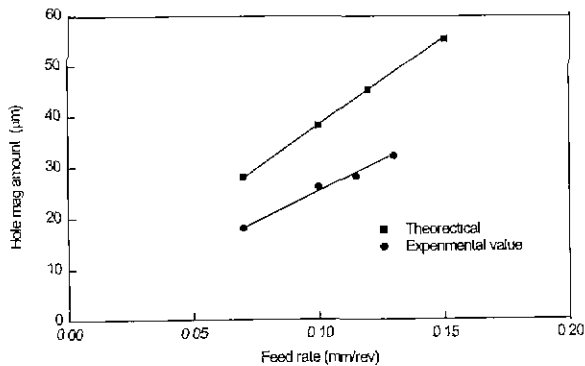


Fig. 16 Influence of feed rate on the amount of hole magnification

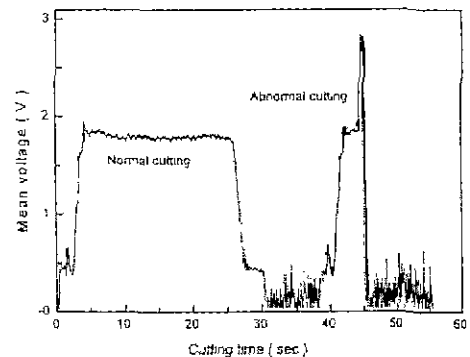


Fig. 19 Variant voltage of BTA drilling on V=70m/min, f = 0.15mm/rev, SM55C⁵⁾

Fig. 19 shows the variant voltage of BTA drilling at cutting speed $V=70\text{m/min}$, feed rate $f = 0.15\text{mm/rev}$.

In this figure, we can evaluate the effect the abnormal cutting region might have a creation of the drill tip wear.⁵⁾

3-6. Chip Curling and Guide Pad Activities

Fig. 20 shows a photograph on the lead end of a BTA drilled workpiece. In this figure, the chip curling appears to be in conical type. The burnishing surface by guide pad activities is shown at points [H] and [I]. At point [H], the drilling surface is in dark color. This suggests that the cutting temperature at the critical outer tip sharpened edge and drilling surface is presumably above 900°C . It is also noted that, along the outer drilling surface line we can measure the lobe profile and chattering phenomena due to BTA-drills instability. The chip curling can be observed at points [C], [E], [G] and the lead end cutting surface, at points [A], [B], [D], [F] is observed along the its traces.

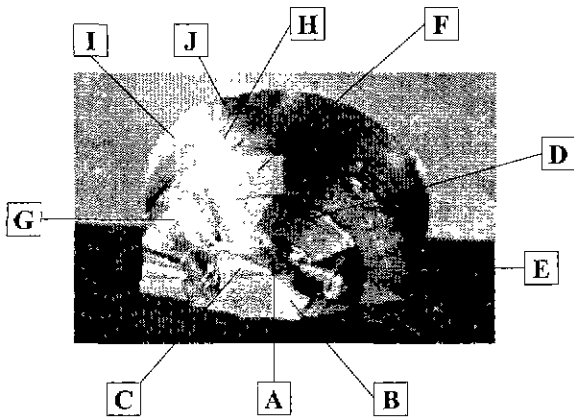


Fig. 20 Photograph on the lead end of BTA drilled workpiece (SM45C VS. P20)

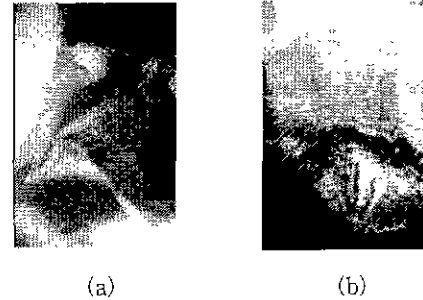
Fig. 21(a) was taken at the point indicated at Fig. 20[G], which is BTA drilled chip curling on SM45C carbon steel on the outer tip. This chip was smooth conical. Similar flow type chip length was observed in the case of three BTA drill tips (outer tip, middle tip and inner tip). For example Fig. 21(b) was taken from Fig. 20[C], which is BTA drilled chip curling on the inner tip.

This chip was in a form of extreme conical type chip curling that had the shortest chip length among all three BTA drill tips.

3-7. Tool Wear and Its Analysis

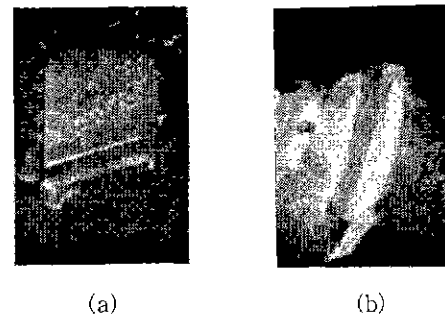
Fig. 22 shows the photographs of BTA drill's tip and guide pad after extreme tool wear occurred on SM45C teal. From this figure, we can see that the wear of drill tips and guide pads was due to extreme friction between the tool acting edge on tool acting surface and the deep drilling hole wall or lead. At this time it is assumed that high temperature is created because there is so much friction energy. As a result of this concern, proper

drilling conditions, coolant, tool alignment, and workpiece set up method etc. are required to reduce unnecessary tool wear.



(a) The chip phenomena from outer tip
(b) The chip phenomena from inner tip

Fig. 21 Phenomena of BTA drilled chip curling result from SM45C carbon steel ($\times 7$)



(a) The extreme wear observed on BTA drill's entire outer tip ($\times 7$)
(b) The extreme wear observed on BTA drill's entire guide pad hole wall contacted surface ($\times 7$)

Fig. 22 Phenomena of BTA drill's tip and guide pad wear(P20)

Fig. 23(a) shows the SEM photograph of the center wear on tool rake surface at BTA drill's outer tip.(drilling condition . SCM440, $\varnothing 19.25$, $V=100\text{m/min}$, $f = 0.18\text{mm/rev}$,)

Fig. 23(b), (c) show the element distribution at point [A] of Fig.23(a)

It is noted that, the amount of Ti is very high among all BTA drills tips used in this study. The cause of this observation is that point [A] does not have much wear, but point [B] experiences the most wear due to friction with drilling chips. At point [B] in Fig. 23(a), it has been estimated by Geoffrey Boothroyd.^{6,9-11)} that the temperature may reach $900\sim 1200^{\circ}\text{C}$ on the carbide tool edge.

Due to the loss of Ti above 900°C generated friction heat,⁵⁾ [B] point tool wear is much more than that at point [A]. This argument is consistent with the observation that the amount of Ti in Fig. 23(b) is less than [A] point in Fig. 23(a).



Fig. 23(a) Material elements distribution at the point A in Fig. 20

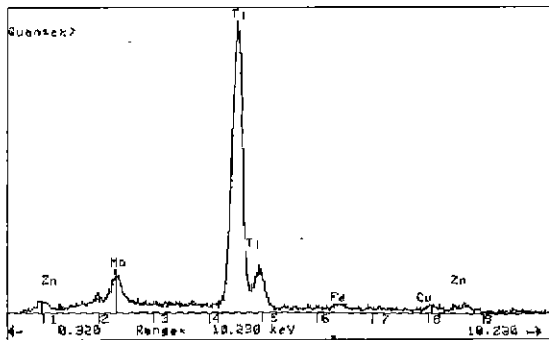


Fig. 23(b) Material elements distribution at the point B in Fig. 20

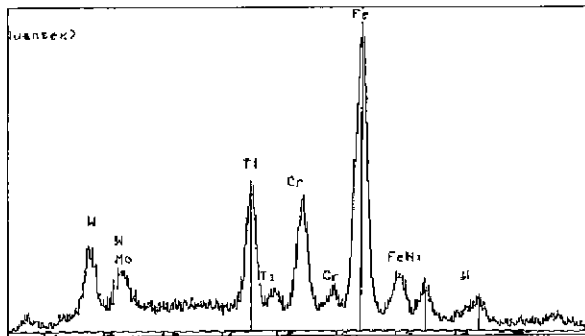


Fig. 23(c) Material elements distribution at the point A in Fig. 20

Conclusions

Experiments have been performed using P20, P30, P70 BTA deep hole drilling.

The tool axis direction used was in accordance with the conditions for CNC deep hole drilling machine for SM45C, SM55C carbon steel, SCM440 alloy steel.

BTA drill diameter of $\varnothing 19.25\text{mm}$ were selected.

The deep hole drilling experiments were performed at various cutting speed, and feed.

Deep hole shape was recorded and analyzed. In addition surface

roughness, straightness, roundness, lobe profile, hole magnification and tool wear were investigated. The conclusions were as follows.

(1) Roughness, straightness, roundness, hole magnification satisfactory for field applications could be obtained with suitable cutting conditions.

(2) The profile of BTA drilled hole displays 2~8 lobes depending on rotating speed and tool axis revolving speed. This phenomena is the same with theoretical calculated graphics.

(3) The wear of BTA drill tips appears in crater, flank and chipping form, and it is associated with a decrease in Ti due to the formation of TiC at the high temperature generated by the friction between tip and workpiece.

Reference

1. H. J. Swinehart, Gun Drilling, Trepanning, & Deephole Machining, ASTM, 1967
2. S. B. Sim, A Study on the Characteristics of Deep Hole Drilling for Carbon Steel, Ph.D thesis, Dept. of Mech. Eng. Graduate school, Dong-A University, Pusan, Korea, pp.1~170, 1995
3. Keizo Sakuma, Koichi Taguchi, Akio Kasuki, Study on Deep - Hole Boring by BTA System Solid Boring Tool, Precision Machine, Vol.44. No 9. pp.69~74, 1978
4. K. Sakuma, K. Taguchi, A. Katsuki, Self-Guiding Action of Deep-Hole-Drilling Tools, Annals of the CIRP, 1981
5. S. G. Chang, A Study on Hole Accuracy Improvement and Condition Monitoring of Tool in Deep Hole Drilling with BTA Drill, Graduate School, Dong-A University, pp.38~126, 1998
6. Kunio Uehare, Keji Nishina, Hideo Takeshita, Kazuya Uchida, On the Mechanism of Crater Were of Carbide Cutting tool in the Region of Low Cutting Speed, Precision Machine, Vol.38, No. 3, pp.261~267, 1972
7. M.O.M. Osman, V. Latinvic, B. Greuner, On the Performance of Cutting Fluid for BTA Deep-Hole Machining, Int. J. Prod. Res., Vol.19, No. 5, pp.491~503, 1981
8. S. B. Sim, T. O. Jun, A Study on the characteristics of BTA Deep Hole Drilling for Marine Part Materials, Proceedings of the seventh Inter. Offshore and Polar Eng. Conference, Vol. IV, pp.798~806, 1997
9. S. B. Sim, T. O. Jun, A Study on the Accuracy of Gun Deep Hole Drilling for Marine Part Materials, Proceedings of the eighth Inter Offshore and Polar Eng. Conference, Vol.1, pp.363~370, 1998
10. S. B. Sim, c. O. Kim, The Hole Profile and Tool wear of BTA Deep Hole Drilling for SUS316 Marin Part Material, Proceeding of the Ninth Inter. Offshore and Polar Eng. Conference, Vol. IV, pp.154~161, 1999